

Young mice administered adult doses of AAV5-hFVIII-SQ achieve therapeutic factor VIII expression into adulthood

Lening Zhang,^{1,5} Bridget Yates,^{1,5} Ryan Murphy,¹ Su Liu,¹ Lin Xie,¹ Britta Handyside,¹ Choong-Ryoul Sihn,¹ Taren Bouwman,¹ Nicole Galicia,¹ Danielle Tan,¹ Carlos Fonck,² Jeremy Arens,³ Annie Clark,³ Weiming Zhang,⁴ Sundeep Chandra,³ Jaydeep Srimani,³ Jennifer Holcomb,³ Andrea Van Tuyl,³ Joshua Henshaw,³ Christian Vettermann,³ Silvia Siso,¹ Cheng Su,⁴ Sherry Bullens,¹ Stuart Bunting,¹ Charles O'Neill,³ and Sylvia Fong¹

¹Biology Research, BioMarin Pharmaceutical Inc., Novato, CA 94949, USA; ²Pharmacological Sciences, BioMarin Pharmaceutical Inc., Novato, CA 94949, USA; ³Translational Sciences, BioMarin Pharmaceutical Inc., Novato, CA 94949, USA; ⁴Data Sciences and Analytics, BioMarin Pharmaceutical Inc., Novato, CA 94949, USA

Valoctocogene roxaparvec (AAV5-hFVIII-SQ) gene transfer provided reduced bleeding for adult clinical trial participants with severe hemophilia A. However, pediatric outcomes are unknown. Using a mouse model of hemophilia A, we investigated the effect of vector dose and age at treatment on transgene production and persistence. We dosed AAV5-hFVIII-SQ to neonatal and adult mice based on body weight or at a fixed dose and assessed human factor VIII-SQ variant (hFVIII-SQ) expression through 16 weeks. AAV5-hFVIII-SQ dosed per body weight in neonatal mice did not result in meaningful plasma hFVIII-SQ protein levels in adulthood. When treated with the same total vector genomes per mouse as adult mice, neonates maintained hFVIII-SQ expression into adulthood, although plasma levels were 3- to 4-fold lower versus mice dosed as adults. Mice <1 week old initially exhibited high hFVIII-SQ plasma levels and maintained meaningful levels into adulthood, despite a partial decline potentially due to age-related body mass and blood volume increases. Spatial transduction patterns differed between mice dosed as neonates versus adults. No features of hepatotoxicity or endoplasmic reticulum stress were observed with dosing at any age. These data suggest that young mice require the same total vector genomes as adult mice to sustain hFVIII-SQ plasma levels.

INTRODUCTION

Hemophilia A (HA) is an X-linked genetic bleeding disorder caused by a deficiency in the activity of coagulation factor VIII (FVIII).^{1,2} Individuals with severe deficiencies (i.e., <1 IU/dL) experience spontaneous bleeding internally into joints or muscles.¹ Hemarthrosis typically develops before 2 years of age in children with severe HA and, if untreated, leads to recurrent bleeds with musculoskeletal deformity and loss of mobility.^{3,4} Thus, effective early pediatric treatment is needed to prevent bleeding, pain, joint damage, and muscle atrophy.^{1,5} Regular prophylactic administration of exogenous FVIII is recommended to prevent anticipated bleeding and

joint destruction, preserve normal musculoskeletal function, and improve quality of life.^{2,6,7} Importantly, treatments that result in modest increases in plasma FVIII levels (i.e., 5–15 IU/dL) may lead to considerable improvements in HA-related clinical outcomes.⁸

Valoctocogene roxaparvec (AAV5-hFVIII-SQ) is an adeno-associated virus (AAV) serotype 5 vector containing a codon-optimized SQ variant of B-domain-deleted human FVIII (hFVIII-SQ) controlled by a liver-selective promoter.⁹ In a phase 1/2 trial, a single administration of AAV5-hFVIII-SQ resulted in clinical improvements in terms of reduced bleeding and FVIII use for up to 5 years in adult men with severe HA.^{9–11} Gene therapy treatment in early life could theoretically achieve therapeutic levels of FVIII by enabling the recipient to produce sufficient FVIII to prevent bleeding.¹²

Previous preclinical research in neonatal mice and non-human primates with AAV vectors indicates robust liver cell proliferation early in life can prevent stable transgene expression.^{13–16} Delaying vector administration may increase the durability of transgene expression.^{13,14} Here, we present results of studies evaluating the preservation of AAV5-hFVIII-SQ vector genomes during growth of young mice, the hepatic transduction patterns and kinetics of hFVIII-SQ expression in neonatal versus adult mice, and the impact of AAV5-hFVIII-SQ treatment on liver function and overall safety, with the key objectives of determining the dose of AAV5-hFVIII-SQ and age at administration required to achieve and maintain meaningful plasma hFVIII-SQ protein levels into adulthood.

Received 13 January 2022; accepted 9 August 2022;
<https://doi.org/10.1016/j.omtm.2022.08.002>.

⁵These authors contributed equally

Correspondence: Sylvia Fong, Biology Research, BioMarin Pharmaceutical Inc., 105 Digital Drive, Novato, CA 94949, USA
E-mail: sfong@bmrn.com



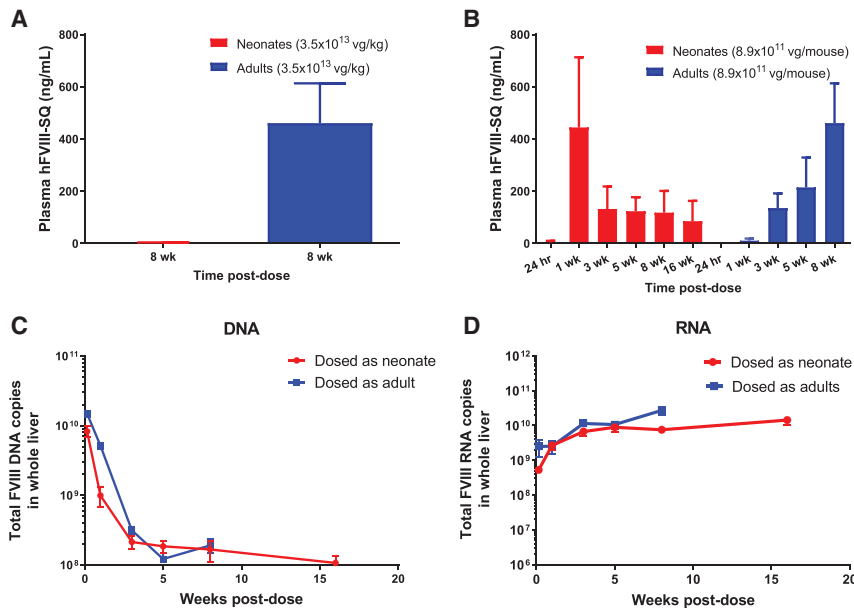


Figure 1. Outcomes following AAV5-hFVIII-SQ treatment in neonates (2 days old) versus adults (8 weeks old).

(A) Plasma hFVIII-SQ levels at 8 weeks post-treatment with AAV5-hFVIII-SQ (3.5×10^{13} vg/kg) in neonates versus adults. (B) hFVIII-SQ protein concentrations in plasma by time point in neonates and adults treated with AAV5-hFVIII-SQ (8.9×10^{11} vg/mouse). (C) Total AAV5-hFVIII-SQ vector genomes in liver by time point in neonates and adults treated with AAV5-hFVIII-SQ (8.9×10^{11} vg/mouse) detected by qPCR. (D) Total hFVIII-SQ RNA in liver by time point in neonates and adults treated with AAV5-hFVIII-SQ (8.9×10^{11} vg/mouse) detected by RT-qPCR. Data are shown as mean \pm standard deviation in red for mice dosed as neonates and blue for mice dosed as adults. AAV5-hFVIII-SQ, adeno-associated virus serotype 5 vector encoding a B-domain-deleted human FVIII; FVIII, factor VIII; hr, hours; PCR, polymerase chain reaction; qPCR, quantitative real-time PCR; RT-qPCR, reverse transcription followed by quantitative real-time PCR; vg, vector genome; wk, weeks.

RESULTS

Dose comparison

Plasma protein production, DNA transduction, and RNA expression

To determine the vector dose needed for newborn mice to achieve and maintain therapeutic FVIII levels when they reach adulthood, neonatal (2 days) and adult (8 weeks) mice received a single intravenous bolus injection of AAV5-hFVIII-SQ. Adult mice were treated with a total dose of 8.9×10^{11} vector genomes (vg) of AAV5-hFVIII-SQ, equivalent to 3.5×10^{13} vg/kg. Neonatal mice received gene transfer at doses of 8.9×10^{11} vg of AAV5-hFVIII-SQ (equivalent to 4.5×10^{14} vg/kg), matching the total number of vector genomes received by adult mice, or 7.2×10^{10} vg per mouse, matching the relative dose level of the adult mice based on body weight (3.5×10^{13} vg/kg). Mice were euthanized at 24 h, 1, 3, 5, 8, or 16 weeks post vector administration (Figure S1A). Levels of liver hFVIII-SQ DNA, RNA and protein, and plasma hFVIII-SQ protein were evaluated.

Gene transfer with AAV5-hFVIII-SQ resulted in the successful production of hFVIII-SQ protein in adult mice. At 8 weeks post dose, adult mice dosed with 3.5×10^{13} vg/kg AAV5-hFVIII-SQ had mean 460.7 ng/mL hFVIII-SQ in plasma (Figure 1A; Table 1). Conversely, neonatal mice treated with AAV5-hFVIII-SQ vector genomes given at the same relative dose level as adult mice when normalized to body weight (3.5×10^{13} vg/kg) did not produce meaningful levels of plasma hFVIII-SQ protein; levels of plasma hFVIII-SQ protein were barely detectable at 8 or 16 weeks after infusion, with mean concentrations of 3.1 ng/mL and 0.6 ng/mL, respectively. Total levels of liver hFVIII-SQ DNA and RNA were consistently much lower for neonates treated with this dose compared with adults. In contrast to the relative dose based on weight, all neonatal mice dosed with the same total number of vector genomes as adults (8.9×10^{11}

vg/mouse) had detectable plasma levels of hFVIII-SQ protein from 1 week (444.6 ng/mL) through 16 weeks post dose (85.5 ng/mL) (Figure 1B; Table 1).

The kinetics of hFVIII-SQ protein levels in plasma differed between neonatal and adult mice dosed with 8.9×10^{11} vg/mouse AAV5-hFVIII-SQ. In adult mice, hFVIII-SQ protein was not detected in circulation until 3 weeks post dose, and plasma levels of hFVIII-SQ showed a time-dependent increase (Table 1). At 8 weeks, the mean \pm standard deviation (SD) level was 460.7 ± 152.4 ng/mL. In neonatal mice, plasma hFVIII-SQ protein levels were highest at 1 week post dose and declined at week 3; this decline may be due in part to blood volume expansion as a result of rapid growth between 1 and 5 weeks of age (Figures 1B and S2). As the mice grew and blood volume increased, hFVIII-SQ protein levels were maintained into adulthood. At 8 weeks, mean \pm SD plasma hFVIII-SQ was 118.21 ± 83.04 ng/mL in the neonatal cohort dosed at 8.9×10^{11} vg/mouse.

Quantitative polymerase chain reaction (qPCR) showed neonatal mouse livers were capable of taking up the same amount of vector genomes as adults when given the same absolute dose (Figure 1C). The majority of total vector genomes in the liver disappeared over the first few weeks following infusion, as expected given typical AAV-vector processing kinetics; however, the slope of decline was similar between young and adult animals, despite liver growth in the neonatal cohort. Although the liver hFVIII-SQ DNA levels were similar between the two cohorts at 8 weeks after dosing, mice dosed as adults expressed 3.6-fold more liver hFVIII-SQ RNA than mice dosed as neonates (Figure 1D). Total mean \pm SD liver hFVIII-SQ RNA in adult mice increased about 11-fold from $2.51 \times 10^9 \pm 4.02 \times 10^9$ copies/liver at 24 h post dose to $2.71 \times 10^{10} \pm 2.17 \times 10^{10}$ copies/liver at 8 weeks

Table 1. Data summary of hFVIII-SQ DNA and RNA in liver and hFVIII-SQ levels in plasma

Age at dosing and dosage	Take-down post injection	hFVIII-SQ DNA, vg/liver	hFVIII-SQ RNA, copies/liver	Plasma hFVIII-SQ protein, ng/mL
Adults dosed at 8 weeks (3.54×10^{13} vg/kg; 8.9×10^{11} vg/mouse)	24 h	$1.48 \times 10^{10} \pm 4.78 \times 10^9$	$2.51 \times 10^9 \pm 4.02 \times 10^9$	0 ± 0
	1 week	$5.16 \times 10^9 \pm 1.65 \times 10^9$	$2.53 \times 10^9 \pm 3.29 \times 10^9$	10.5 ± 8.2
	3 weeks	$3.14 \times 10^8 \pm 1.35 \times 10^8$	$1.15 \times 10^{10} \pm 3.74 \times 10^9$	135.7 ± 56.0
	5 weeks	$1.22 \times 10^8 \pm 8.81 \times 10^7$	$9.42 \times 10^9 \pm 6.51 \times 10^9$	214.7 ± 114.5
	8 weeks	$1.91 \times 10^8 \pm 1.33 \times 10^8$	$2.71 \times 10^{10} \pm 2.17 \times 10^{10}$	460.7 ± 152.4
Neonates dosed at 2 days (4.47×10^{14} vg/kg; 8.9×10^{11} vg/mouse)	24 h	$8.30 \times 10^9 \pm 4.58 \times 10^9$	$5.30 \times 10^8 \pm 1.18 \times 10^8$	3.9 ± 6.6
	1 week	$9.94 \times 10^8 \pm 9.81 \times 10^8$	$2.66 \times 10^9 \pm 2.05 \times 10^9$	444.6 ± 268.3
	3 weeks	$2.13 \times 10^8 \pm 1.45 \times 10^8$	$6.71 \times 10^9 \pm 5.71 \times 10^9$	131.9 ± 86.2
	5 weeks	$1.85 \times 10^8 \pm 1.17 \times 10^8$	$8.93 \times 10^9 \pm 7.50 \times 10^9$	123.4 ± 53.6
	8 weeks	$1.67 \times 10^8 \pm 1.77 \times 10^8$	$7.54 \times 10^9 \pm 5.02 \times 10^9$	118.2 ± 83.0
Neonates dosed at 2 days (3.54×10^{13} vg/kg; 7.2×10^{10} vg/mouse)	8 weeks	$1.05 \times 10^6 \pm 1.42 \times 10^6$	$9.17 \times 10^7 \pm 6.32 \times 10^7$	3.1 ± 2.9
	16 weeks	$6.12 \times 10^5 \pm 1.94 \times 10^6$	$4.53 \times 10^7 \pm 4.34 \times 10^7$	0.6 ± 1.2

Data are mean \pm SD. Study design is shown in Figure S1A. hFVIII-SQ, human factor VIII SQ variant; SD, standard deviation; vg, vector genome.

post dose (Table 1). Similarly, total mean liver hFVIII-SQ RNA in neonatal mice given the same total vector genomes increased about 14-fold from $5.3 \times 10^8 \pm 1.18 \times 10^8$ at 24 h post dose to $7.54 \times 10^9 \pm 5.02 \times 10^9$ copies/liver at 8 weeks post dose.

Protein production and secretion

We next evaluated potential differences in transgene protein production and secretion in the neonatal versus adult cohorts. First, we calculated the total amount of circulating hFVIII-SQ protein. At 8 weeks post dose, adult mice had approximately 5.6-fold greater total circulating hFVIII-SQ than neonatal mice (mean \pm SD, 1.337 ± 0.460 μ g versus 0.241 ± 0.161 μ g, respectively) (Figure 2A). In liver homogenate, hFVIII-SQ protein was also higher in adult mice, with 2.2-fold more hFVIII-SQ compared with the neonatal cohort (mean \pm SD, 0.754 ± 0.447 μ g versus 0.347 ± 0.197 μ g, respectively) (Figure 2B). When circulating and liver hFVIII-SQ were combined, total protein production was 3.6-fold higher in the adult mice (Figure 2C), consistent with the difference in total levels of liver hFVIII-SQ RNA. Approximately 60% of total hFVIII-SQ protein pro-

duced was secreted in the adult cohort, whereas only 40% was secreted in the neonatal cohort (Figure 2D). These data demonstrate that, when treated with the same number of vector genomes, adult mice both produce and secrete more hFVIII-SQ than mice infused as neonates.

Spatial patterns of liver transduction

Given that both neonate and adult cohorts retained similar levels of hFVIII-SQ DNA at 8 weeks post dose, one hypothesis for reduced RNA/protein production and secretion could be differences in the location of transduced hepatocytes within the hepatic lobule and number of hepatocytes transduced. Previous reports show that AAV5 preferentially transduces adult murine hepatocytes surrounding the central hepatic vein (zone 3 of the hepatic lobule).¹⁷ Evaluations using *in situ* hybridization and immunohistochemistry (IHC) showed that transduction patterns differed between neonatal and adult mice when given the same absolute vector genomes at 8 weeks post dose. In the livers of adult mice, hFVIII-SQ vector genome DNA and protein were distributed in a peri-central pattern; neonatal mice showed no preferential pattern in spatial distribution of transduction for either DNA or protein (Figure 3A). At 8 weeks post dose, 39.7% of hepatocytes in adult mice stained positive for hFVIII-SQ vector DNA compared with only 11.5% of hepatocytes in neonatal mice (Figure 3B). Similarly, at 8 weeks post dose, the total number of hepatocytes immunopositive for hFVIII-SQ protein was lower in neonatal mice when compared with adults, although the difference was not statistically significant (Figure 3C).

Kinetics of vector genome trafficking

We assessed the kinetics of vector genome trafficking in neonatal and adult mice to identify differences that could contribute to the differing levels of vector genome DNA and protein. At 24 h after dosing, on average, more than 92% of hepatocytes in neonates stained positive for hFVIII-SQ vector DNA, compared with only 33% of hepatocytes in the adult cohort at 24 h (Figures 4A and 4B). When looking specifically at the nucleus, vector genomes were detected in 88% of hepatocyte nuclei in neonatal mice and 17% of hepatocyte nuclei in adult mice at 24 h after dosing (Figures 4A and 4C). In adults, the percentage of nuclei staining positive for vector DNA increased to approximately 50% at 3 weeks post dose; in the neonatal cohort, a decline of percentage of nuclei and cells staining positive for vector genome per field of view from 1 week on was observed, suggesting there are mechanisms to degrade vector DNA in the nuclei as well.

Similar to vector genome DNA, hepatocytic hFVIII-SQ protein-positive signals were detected 1-week post dose with no apparent distribution pattern in mice infused as neonates (Figure 4D). In adult mice, hFVIII-SQ protein was not detected until 3 weeks post dose and was only present in hepatocytes surrounding the central veins. In neonatal mice, the total number of hepatocytes immunopositive for hFVIII-SQ protein decreased from 1 to 3 weeks post dose by 42% (not significant) and remained constant through 8 weeks. In adult mice, little to no hFVIII-SQ protein was detected at 1 week post dose (data not shown),

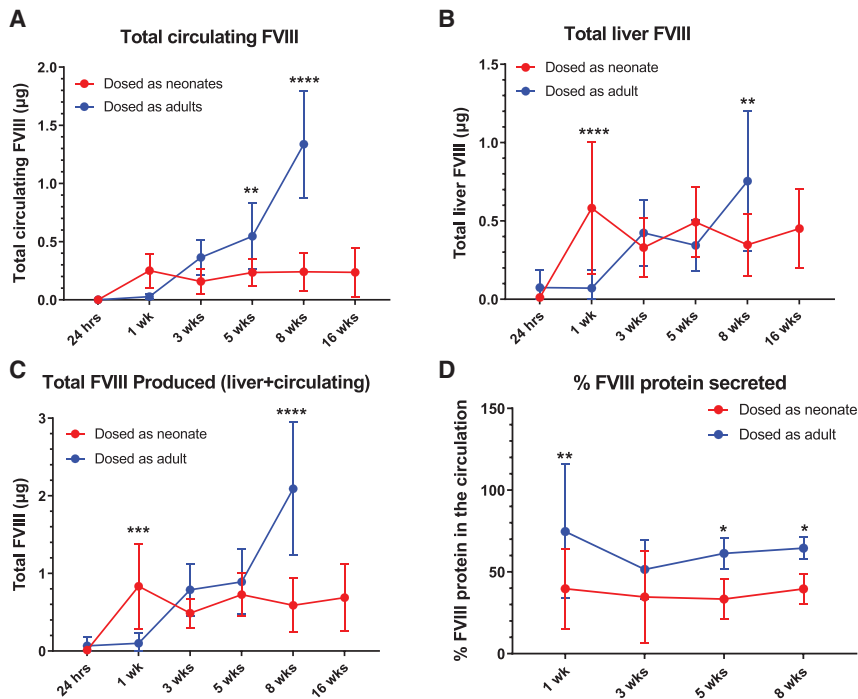


Figure 2. hFVIII-SQ protein production and secretion in mice treated with AAV5-hFVIII-SQ as neonates versus adults

Neonates (2 days old) and adults (8 weeks old) were administered AAV5-hFVIII-SQ 8.9×10^{11} vg/mouse. (A) Total circulating plasma hFVIII-SQ protein by time point following AAV5-hFVIII-SQ treatment. (B) Total hFVIII-SQ protein levels in liver by time point. (C) Total hFVIII-SQ protein in liver and in circulation by time point. (D) Proportion of secreted hFVIII-SQ protein by time point. * $p < 0.05$; ** $p < 0.01$; *** $p < 0.001$; **** $p < 0.0001$. Data are shown as mean \pm standard deviation in red for mice dosed as neonates and blue for mice dosed as adults. Significance was assessed with a two-way ANOVA using a Sidak's multiple comparisons test. AAV5-hFVIII-SQ, adeno-associated virus serotype 5 vector encoding a B-domain-deleted human FVIII; ANOVA, analysis of variance; FVIII, factor VIII; hrs, hour; vg, vector genome; wks, week.

Vector genome structures

We investigated whether there was a difference in the structure of circular vector genomes post dose in mice dosed either as neonates or as adults.¹⁸

DNA samples were treated with Plasmid-Safe DNase (PS-DNase) to enrich for circular episomal genomes, and then additional samples were also treated with the restriction enzyme KpnI to separate individual full-length vector genome units within concatemeric episomes (Figure S4A).¹⁸ Droplet digital PCR (ddPCR) was then used to quantify the count of circular full-length vector genome units per sample, allowing for the identification of concatemeric episomal structures. As expected, circular full-length vector genomes were present at 8 weeks post dose in both mice treated as adults and those treated as neonates with similar levels of vector genomes per diploid genome (Figure S4B). By comparing the numbers of circular genomes upon KpnI treatment, we determined that the extent of concatemericization was similar between mice dosed with AAV5-hFVIII-SQ as adults and as neonates (Figure S4C). Finally, Southern blotting showed that the forms of vector genomes at 8 weeks post dose were also similar between the two groups, with circular episomal genomes present in monomeric, dimeric, and trimeric forms, primarily in head-to-tail configurations (Figure S4D).

Endoplasmic reticulum stress and hepatotoxicity

Biomarkers of hepatotoxicity and endoplasmic reticulum (ER) stress were evaluated after treatment with the same absolute dose (i.e., 8.9×10^{11} vg/mouse) of AAV5-hFVIII-SQ in neonatal and adult mice. There was no increase in glucose-regulated protein 78 (GRP78) expression in hepatocytes expressing hFVIII-SQ in either the adult or neonatal cohort (Figure 5A). Quantification of GRP78 intensity was performed and no difference was detected between neonatal and adult mice (data not shown). In addition, no significant increase in alanine aminotransferase was detected in either cohort, including between neonatal mice that received the higher dose (Figure 5B).

and the total number of hepatocytes staining positive for hFVIII-SQ protein increased ~ 3 -fold from week 3 to week 8 post dose (not significant) (Figure 4E). At 8 weeks post dose, hepatocytes in mice infused as neonates had similar IHC intensity compared with the adult cohort (Figure 4F).

Since hepatocytes within the neonatal mouse liver are smaller (Figure S3) and more densely packed than those of the adult liver, one field of view of the neonate liver represents a greater portion of the total liver than in the adult liver. To account for that difference in cell density per field, we determined the total number of transduced hepatocytes in the whole liver by using liver weight and volume per field. At all time points, significantly more hepatocytes (4- to 7-fold) stained positive in the adult cohort compared with the neonatal cohort (Figure 4G). Despite significant liver weight increases in neonatal mice (Figure S2), the total number of hepatocytes that stained positive for hFVIII-SQ DNA remained stable; the total number of positive hepatocytes was also stable in adult mouse liver. Histological analyses on liver growth in mice determined that hepatocyte mitosis occurred up to 1 week of age, while increases in hepatocyte cell size were observed by 3 weeks of age and onward (Figure S3). In both cohorts, the rate of decline in total vector genomes over time as assessed by *in situ* hybridization intensity was similar and differences were not significant (Figure 4H), which is consistent with the qPCR result. Of note, greater hybridization intensity per hepatocyte was detected in mice infused as neonates compared with adults (Figure 4I). At 8 weeks post dosing, hepatocytes from the neonatal cohort had 5.5-fold higher hybridization intensity than the adult cohort, suggesting higher vector DNA on a per-cell basis.

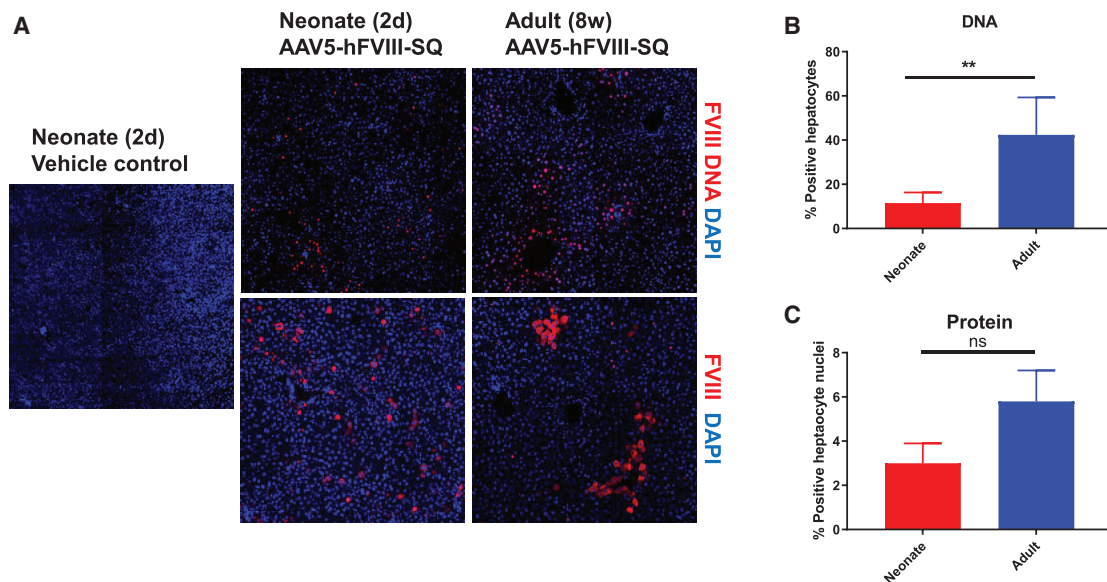


Figure 3. Transduction patterns of AAV5-hFVIII-SQ between mice dosed as neonates versus adults

Neonates (2 days old) and adults (8 weeks old) were administered AAV5-hFVIII-SQ 8.9×10^{11} vg/mouse. (A) Distribution of AAV5-hFVIII-SQ genomes at 8 weeks post treatment in mice dosed at 2 days and 8 weeks of age using *in situ* hybridization (upper) and hFVIII protein by immunohistochemistry (lower). (B) Percentage of hepatocyte transduction in a field $678.8 \mu\text{m}^2$ assessed by *in situ* hybridization at 8 weeks. (C) Percentage of hepatocyte staining positive for hFVIII protein in a field $678.8 \mu\text{m}^2$ at 8 weeks. **** $p < 0.0001$; *** $p < 0.001$; ** $p < 0.01$; ns, not significant. The vehicle control was stained for both human FVIII protein with immunohistochemistry and hFVIII-SQ DNA using dual *in situ* hybridization. DAPI staining shows cell nuclei. For (B) and (C), data are mean \pm standard deviation for number of hepatocytes staining positive for hFVIII DNA and protein in the neonatal (red) versus adult (blue) cohorts, respectively. AAV5-hFVIII-SQ, adeno-associated virus serotype 5 vector encoding a B-domain-deleted human FVIII; d, day; DAPI, 4',6-diamidino-2-phenylindole; FVIII, factor VIII; vg, vector genome; w, week.

Optimal age for AAV5-hFVIII-SQ administration

To determine the effect of age at time of treatment with AAV5-hFVIII-SQ, mice aged 2, 4, 6, and 8 weeks were treated with approximately 1×10^{12} vg of AAV5-hFVIII-SQ per mouse, which corresponded to a weight-based dose level of 1.5×10^{14} , 8.7×10^{13} , 6.5×10^{13} , and 6×10^{13} vg/kg, respectively (Figure S1B). In addition, mice aged 7 days were administered 7.5×10^{11} vg per mouse, which corresponded to 2.0×10^{14} vg/kg. Plasma hFVIII-SQ protein concentrations were measured 1, 2, 4, or 12 weeks post dose. Consistent with results in neonates, mice dosed at 1 week old exhibited high plasma protein concentrations at 1 week post dose, which declined by 2 weeks post dose and remained at steady state for the remainder of the study (Figure 6A). In mice dosed at ages 2, 4, 6, and 8 weeks, plasma hFVIII-SQ protein concentrations increased over 12 weeks, consistent with previous results in the adult cohort. At 12 weeks post dose, mean plasma hFVIII-SQ concentrations in mice dosed at 1, 2, 4, 6, and 8 weeks were 126 ± 152 , 92 ± 32 , 207 ± 135 , 367 ± 240 , and 294 ± 174 ng/mL, respectively. At 12 weeks, levels of total liver hFVIII-SQ DNA were significantly lower in mice dosed at 1 and 2 weeks old compared with those dosed at 4 weeks and older (Figure 6B), and hFVIII-SQ RNA was highest in mice dosed at 4 weeks, slightly higher than in mice dosed at 1, 2, or 8 weeks, although the difference was statistically significant (Figure 6C). At 12 weeks, mean FVIII activity in plasma was highest in mice dosed at 6 weeks, but only slightly higher than the other timepoints, with the difference being significant only compared with mice dosed at

2 weeks (Figure 6D). Additionally, AAV5-hFVIII-SQ administration at any age did not result in any treatment-related mortality, clinical observations, body weight changes, clinical chemistry changes, or gross or microscopic findings.

Overall, at 12 weeks post dose, mice that were dosed at the age of 1 or 2 weeks had lower plasma hFVIII-SQ, total hFVIII-SQ DNA, and FVIII activity compared with mice dosed at 6 or 8 weeks. The optimal age to administer AAV5-FVIII-SQ in mice may be 4 weeks or older as these mice had higher plasma hFVIII-SQ concentration and FVIII activity; however, younger mice still achieved considerable plasma hFVIII-SQ levels into adulthood.

DISCUSSION

This is the first study to evaluate AAV5-hFVIII-SQ neonatal dosing and to model the kinetics of hFVIII-SQ gene and protein expression in neonatal versus adult mice. The results demonstrate that the capacity for AAV5-hFVIII-SQ transduction and rate of DNA decline in neonatal mouse liver are comparable with adult mouse liver when administered the same total quantity of AAV5-hFVIII-SQ.

When treated with the same absolute dose, young mice (<1 week) and adult mouse livers had generally similar hFVIII-SQ DNA levels; however, adult mouse livers produced and secreted more hFVIII-SQ protein than young mice and had approximately 3- to 4-fold higher

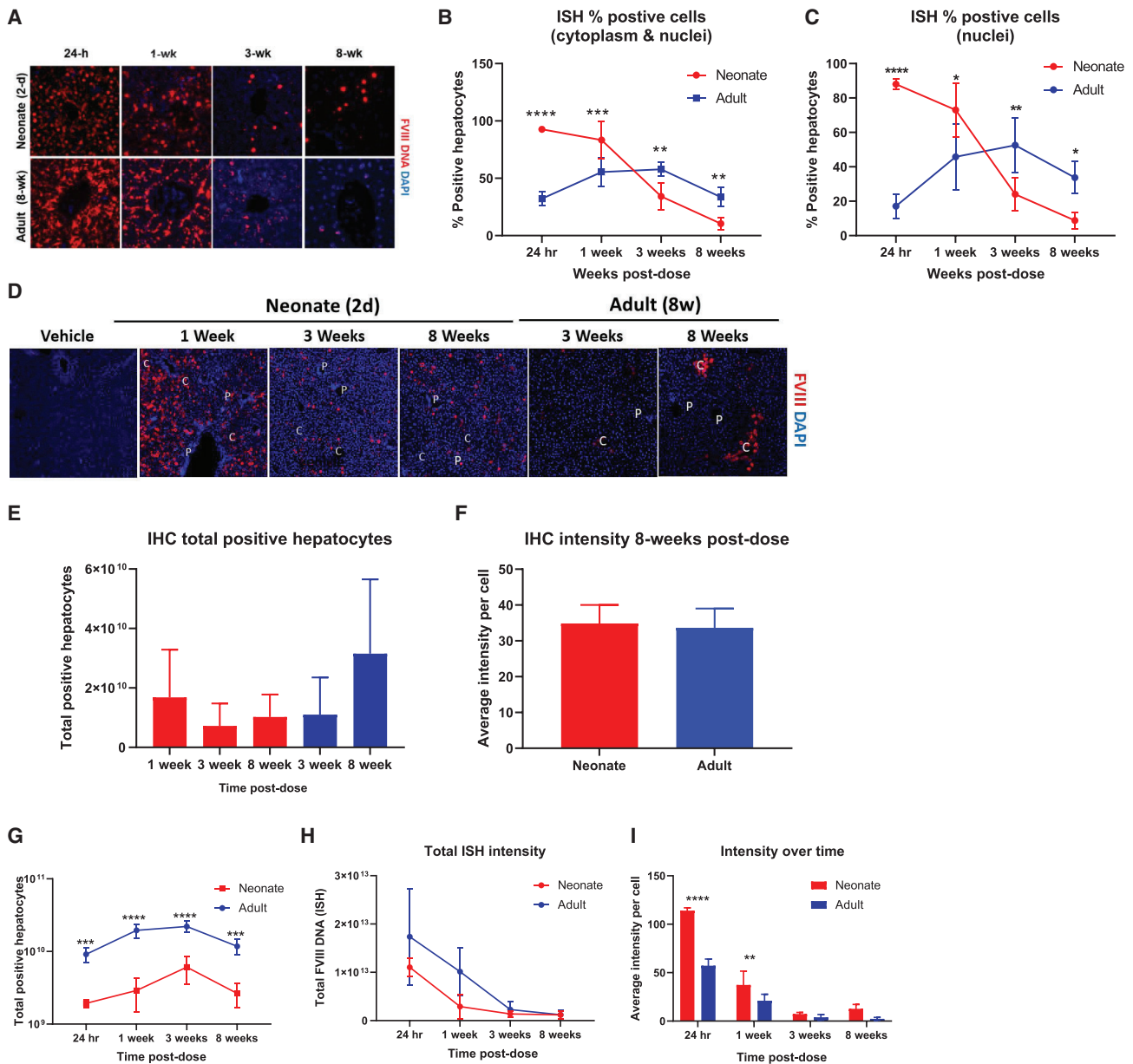


Figure 4. Kinetics of AAV5-FVIII-SQ trafficking and expression. Neonates (2 days old) and adults (8 weeks old) were administered AAV5-hFVIII-SQ 8.9×10^{11} vg/mouse

(A) Hepatocellular staining of hFVIII DNA in hepatocytes over time. (B) Percentage of hepatocyte stained positive for hFVIII DNA in cytoplasm or nuclei per $678.8 \mu\text{m}^2$ field assessed by *in situ* hybridization over 8 weeks. (C) Percentage of hepatocytes stained positive for hFVIII DNA in the nucleus per $678.8 \mu\text{m}^2$ area assessed by *in situ* hybridization over 8 weeks. (D) Hepatocellular distribution of hFVIII protein over 8 weeks per immunohistochemistry. (E) Total number of hepatocytes that stained positive for AAV5-hFVIII-SQ protein over 8 weeks. (F) Average hFVIII-SQ protein intensity per cell at 8 weeks post dose. (G) Total number of hepatocytes in whole liver that stained positive for AAV5-hFVIII-SQ DNA over 8 weeks. (H) Total hFVIII-SQ DNA intensity in whole liver over 8 weeks. (I) hFVIII-SQ DNA intensity per cell over 8 weeks. **** $p < 0.0001$; *** $p < 0.001$; ** $p < 0.01$; ns, not significant. Data are shown as mean \pm standard deviation in red for mice dosed as neonates and blue for mice dosed as adults. In (D), the 8-week images of neonatal and adult samples are also shown in Figure 3A. AAV5-hFVIII-SQ, adeno-associated virus serotype 5 vector encoding a B-domain-deleted human FVIII; C, central vein; DAPI, 4',6-diamidino-2-phenylindole; FVIII, factor VIII; hr, hour; IHC, immunohistochemistry; ISH, *in situ* hybridization; wk, week; P, portal vein.

plasma levels compared with young mice when they reached the same age in adulthood. Young mice (≤ 1 week of age) dosed with the same total vector genomes as adult mice initially had very high circulating

hFVIII-SQ protein levels. These levels declined rapidly as the mice grew and blood volume increased, although resultant circulating hFVIII-SQ protein levels remained substantial. In contrast, when

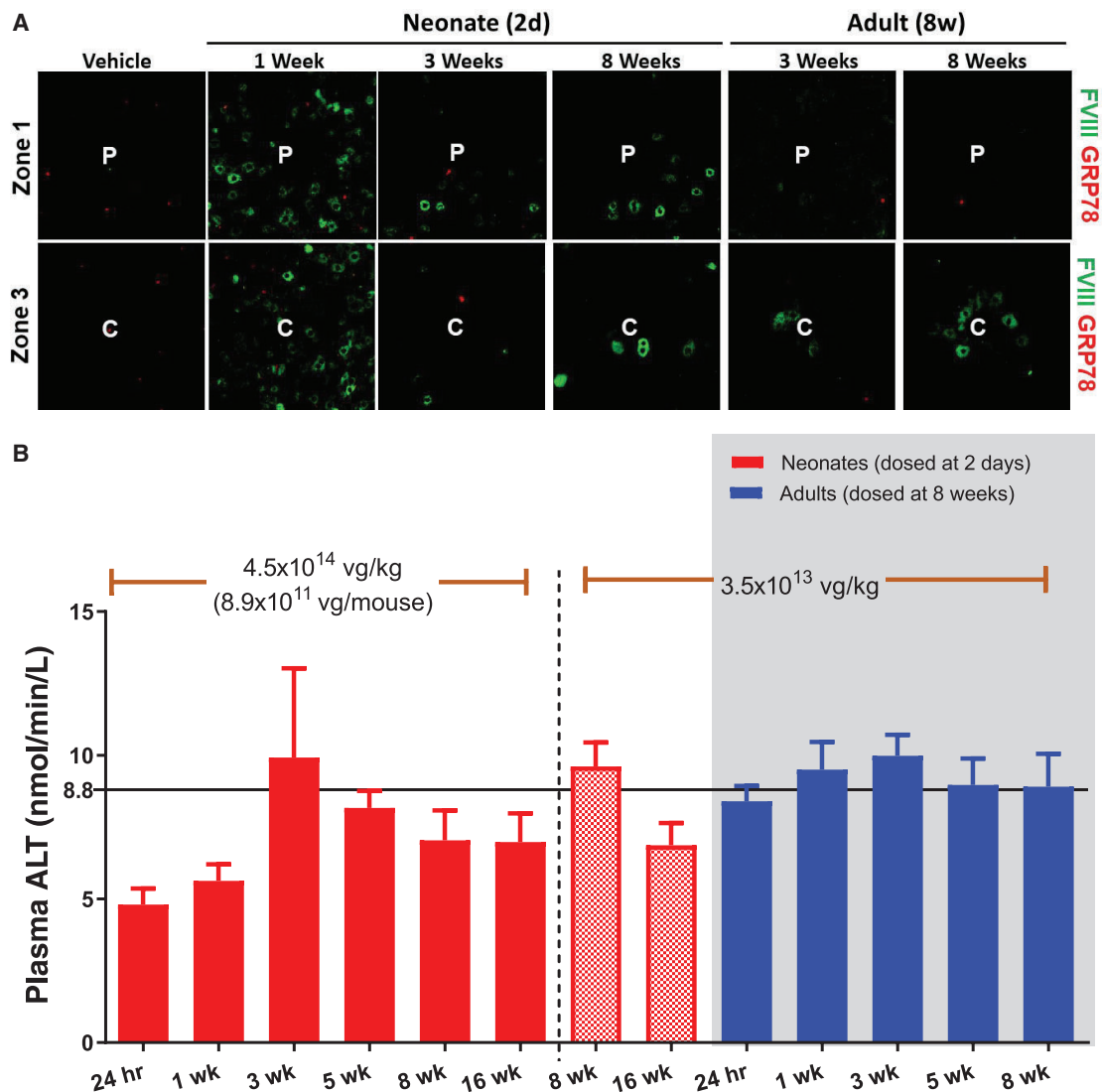


Figure 5. AAV5-hFVIII-SQ does not induce hepatotoxicity. Neonates (2 days old) and adults (8 weeks old) were administered AAV5-hFVIII-SQ 8.9×10^{11} vg/mouse

(A) Immunohistochemistry for GRP78 expression in hepatocytes by time point following AAV5-hFVIII-SQ dosing. (B) Fluorometric assay for alanine aminotransferase levels by time point following AAV5-hFVIII-SQ dosing at 8.9×10^{11} per mouse or 3.5×10^{13} vg/kg. Data are shown as mean \pm standard deviation. The average ALT in animals dosed with vehicle was 8.8 nmol/min/L, as indicated with a solid black line in Figure 5B. AAV5-hFVIII-SQ, adeno-associated virus serotype 5 vector encoding a B-domain-deleted human FVIII; ALT, alanine aminotransferase; C, central vein; d, day; FVIII, factor VIII; GRP78, 78 kDa glucose-regulated protein; P, portal vein; vg, vector genomes; wk, week.

neonatal mice were administered the same per-body-weight dose as adult mice, the majority of animals had undetectable circulating hFVIII-SQ protein levels when they reached adulthood. Together, these data demonstrate that young mice can achieve and maintain therapeutically meaningful FVIII expression into adulthood when treated with the same absolute number of AAV5-hFVIII-SQ vector genomes as adult mice.

The two doses evaluated differed about 10-fold in total vector genomes administered. Neonatal doses were chosen to avoid exceeding

the total vector genome dose in adults and to use only those already clinically validated in adult human participants with a good safety profile. The total liver hFVIII-SQ genomes in neonates 8 or 16 weeks post dose with the same total vector genomes were about 100- to 200-fold higher compared with neonates dosed by body weight, respectively. This greater-than-dose-proportional response was observed previously in mice and in humans.^{10,17,19} In a phase 1/2 trial with AAV5-hFVIII-SQ, mean hFVIII-SQ activity and protein levels increased greater than proportional to dose between 4×10^{13} vg/kg and 6×10^{13} vg/kg. This is because successful transduction of AAV

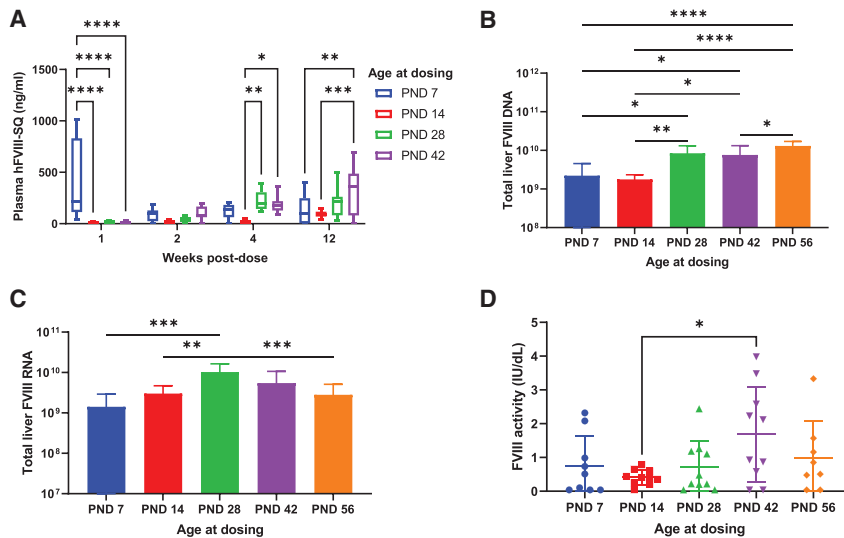


Figure 6. AAV5-hFVIII-SQ expression in mice of different ages. Mice aged 7, 14, 28, 42, and 56 days (n = 10 per group) were infused with AAV5-hFVIII-SQ

(A) Plasma hFVIII-SQ levels in mice after treatment with AAV5-hFVIII-SQ. (B) Total liver hFVIII-SQ DNA in mice after treatment with AAV5-hFVIII-SQ. (C) Total liver hFVIII-SQ RNA in mice after treatment with AAV5-hFVIII-SQ. (D) hFVIII activity in mice after treatment with AAV5-hFVIII-SQ. * $p < 0.05$; ** $p < 0.01$; *** $p < 0.001$; **** $p < 0.0001$. In (A) boxes represent the median and interquartile range and whiskers represent the minimum and maximum, and significance was assessed with a two-way ANOVA using a Tukey's multiple comparison test; in (B)–(D), data are shown as mean \pm standard deviation and significance was assessed with a one-way ANOVA using a Tukey's multiple comparison. AAV5-hFVIII-SQ, adeno-associated virus serotype 5 vector encoding a B-domain-deleted human FVIII; ANOVA, analysis of variance; FVIII, factor VIII; PND, post-natal day.

containing this oversized vector expression cassette consisting of a single-stranded DNA molecule requires either second-strand synthesis or annealing of the positive and negative strands of vector genome and subsequent repair within the same cell.^{20–23} Only repaired, double-stranded, full-length genomes are functional and capable of making hFVIII-SQ RNA and protein, and for oversized vector genomes, such as the one used in this study, conversion from single-stranded DNA to double-stranded DNA may be carried out by multiple processes.^{21,23} Therefore, for a given dose of vectors, half of the vectors would be positive strands and half would be negative strands. If we assume a rate of transduction $v = k * c(A) * c(B)$, where $c(A)$ is the concentration of positive strands, and $c(B)$ is the concentration of negative strands (k is a constant), then, for a 10-fold difference in vector doses administered, the transduction rate would have a theoretical 100-fold difference (i.e., the second power of the vector concentration difference), thus exhibiting a greater-than-dose-proportional response pattern.

Although neonatal and adult mice had similar levels of total liver hFVIII-SQ vector genomes at 8 weeks post dose, mice dosed as neonates had a lower total number of hepatocytes that stained positive for hFVIII-SQ DNA. This suggests that transduced hepatocytes contained more copies of hFVIII-SQ genomes per hepatocyte, which could result in higher expression of hFVIII-SQ RNA and protein per hepatocyte. However, the high hFVIII-SQ DNA concentration in liver did not result in increased protein production, suggesting that there may be a limit to the amount of protein that neonatal and adult hepatocytes can produce and secrete in response to AAV5-hFVIII-SQ transduction. It is interesting that transduced hepatocytes of neonatal mice appeared to secrete 2.2-fold lower amounts of hFVIII-SQ protein than transduced hepatocytes of adult mice. Of note, there was no evidence of ER stress induced in mice treated with AAV5-hFVIII-SQ as neonates, as there was no elevation in the percent of cells that stained positive for GRP78 protein. These results are consistent with a previous

study assessing the administration of AAV5-hFVIII-SQ to adult hemophilic mice.^{17,24} In that study, AAV5-hFVIII-SQ administration resulted in dose-dependent increases in hFVIII-SQ RNA and DNA, therapeutic levels of hFVIII-SQ protein, and decreased bleeding with no induction of ER stress or apoptosis. The weaker promoter used in AAV5-hFVIII-SQ may reduce the likelihood of hFVIII-SQ overproduction per cell, thus limiting induction of the unfolded protein response.

There were also differences in the pattern of transduction and kinetics of AAV5-hFVIII-SQ trafficking and of hFVIII-SQ protein expression in the liver. Neonatal mice showed no clear pattern of transduction versus a pericentral pattern in adult mice. Further, hFVIII-SQ vector genome can be detected in hepatocyte nuclei of neonatal mice by 24 h post AAV5-hFVIII-SQ treatment compared with a delay of 3 to 8 weeks for adult mice, which may explain the more rapid expression of hFVIII-SQ protein observed in the younger mice. Differences in hFVIII-SQ RNA and protein production, as well as protein secretion, may explain the lower level of plasma hFVIII-SQ protein in younger mice versus adult mice. It is possible that adults secrete more hFVIII-SQ protein because more cells are transduced or that pericentral (zone 3) hepatocytes expressing hFVIII-SQ are better able to secrete hFVIII-SQ protein.²⁵

In the neonatal cohort, the proportion of cells staining positive for hFVIII-SQ DNA declined beyond 1 week post dose. It is unlikely that such reduction in percentage positive vector staining is the result of hyperplastic hepatocyte proliferation/division during this phase, since the incidence of mitotic hepatocytes was close to 0% at 1 week of age and not detected at older ages (Figure S3C). Therefore, the loss of genomes observed in mice dosed at 2 days may be in part due to liver growth via cell division only during the first week of life, but not after. The dramatic increase in hepatocyte area detected from 1 week of age onward suggests that the mouse liver is growing primarily by hypertrophy beyond 1 week (Figure S3B). Similarly, previous

studies have shown that very little proliferation occurs after birth under normal circumstances (i.e., without injury).^{26,27} Loss of vector genomes after week 1 must therefore be due to other mechanisms, such as the innate cellular immune response against viral DNA. The novel finding that total number of transduced hepatocytes remained stable from 24 h to 8 weeks treatment in the neonatal cohort (Figure 4D) suggests that hFVIII-SQ vector genomes are not lost due to hepatocyte mitosis in neonates. Rather, the *in situ* hybridization staining intensity per cell decreased over time for both the neonatal and adult cohorts, suggesting that the degradation of vector genomes in each transduced hepatocyte contributed to the overall loss of vector genomes.

While previously published preclinical studies have typically assessed liver-specific AAV-targeted treatment in young animals on a per-body-weight basis,^{14,28,29} here we demonstrate that treating young mice with the same adult vector genome dose of AAV5-hFVIII-SQ results in production and maintenance of therapeutically meaningful levels of circulating hFVIII-SQ when they reach adulthood. Due to their relatively small body size and low blood volume, an initial high level of circulating hFVIII-SQ that could pose a risk of thromboembolic events would be unavoidable in young mice treated with an adult dose of AAV5-hFVIII-SQ. However, the high concentration of circulating hFVIII-SQ is expected to be diluted over time as the body grows and blood volume increases. The long-term duration of clinically meaningful levels of hFVIII remains to be determined. Further, although therapeutic levels of hFVIII were achieved in young mice (≤ 1 week old), careful evaluation is needed to determine whether the initially high levels of hFVIII in neonates poses a safety risk.

A key limitation of this study is that the results from mouse models may not be generalizable to humans. Studies evaluating liver-directed AAV gene transfer in rhesus monkeys, which have a growth trajectory more similar to humans, showed different relationships between dose-timing and transduction patterns than those observed in mice.¹⁴ While AAV gene transfer in infant monkey liver also results in unstable gene transfer and transduction, delaying the age of vector administration in rhesus monkeys from 1 week to 1 month did not improve transduction efficiency.¹⁴ Although the molecular mechanisms of aging are similar between mice, rhesus monkeys, and humans, mice have shorter lifespans and an accelerated early life period. This study did not assess functional outcomes. Comparing rates of genomic integration in animals dosed as neonates versus those dosed as adults would also be valuable, but we believe such comparisons would be more meaningful in a mouse model with a humanized liver, as typical AAV genomic integration locations differ between mice and primates.^{30–33}

In conclusion, this study suggests that administration of AAV5-hFVIII-SQ in younger subjects is feasible but may require the same absolute quantity of vector genomes as used in adults to achieve therapeutically meaningful levels of hFVIII-SQ into adulthood. Further evaluation of this promising therapeutic approach, including safety parameters, merits continued investigation.

MATERIALS AND METHODS

Study conduct

The studies were conducted by the Translational Biology Department of BioMarin Pharmaceutical, at the Buck Institute (Novato, CA), and at Charles River Laboratories (Horsham, PA). Animal breeding and experimental protocols were approved by the Institutional Animal Care and Use Committees of the Buck Institute and Charles River Laboratories.

Vector production

As the full-length hFVIII protein is too large to be packaged into AAV capsids and has poor cellular expression, the vector was modified to improve expression.^{17,34} The AAV5-hFVIII-SQ vector contains a ~ 4.9 -kb genome with the sequence including double-stranded inverted terminal repeats at the 5' and 3' ends, single-stranded DNA encoding a hybrid human liver-selective promoter, a B-domain-deleted human factor VIII cDNA, and a synthetic polyadenylation signal. Further, the hFVIII A2 and A3 domains are linked by a 14-amino acid DNA sequence from the B domain that contains a furin cleavage site (hFVIII-SQ variant).¹⁷

Animals

RAG2^{-/-} (B6.129S6-Rag2^{tm1Fwa}N12; Taconic) \times FVIII^{-/-} (B6.129S-F8^{tm1Kaz}/J; Jackson Laboratories) double-knockout (DKO) mice were used in the study. FVIII^{-/-} mice are homozygous for a targeted, X chromosome-linked mutant allele. Homozygous females and carrier males have less than 1% of normal mouse FVIII activity, exhibit prolonged clotting times, and recapitulate the bleeding phenotype of human HA. The RAG2^{-/-} mouse contains a disruption of the RAG2, which prevents homozygous mice from initiating V(D)J rearrangement and generating mature T or B lymphocytes, minimizing the chance of antibody production against foreign protein. Thus, DKO mice were used to allow assessment of transgene-produced hFVIII-SQ levels without interference of anti-human FVIII antibody formation, as we observed anti-hFVIII antibodies in wild-type mice after 4 weeks.¹⁷ For these studies, RAG2^{-/-} mice, DKO mice, or wild-type mice (C57BL/6J; Jackson Laboratories) were used as the test animals. DKO mice were bred in house, established by breeding male RAG2^{-/-} with female FVIII^{-/-} to generate the first filial generation of heterozygotes. Mating first filial mice yielded mice homozygous for both mutations at a frequency approximating one in eight offspring. Male and female DKO mice were mated to each other to stably propagate the line.

The mice were housed in Makrolon cages with microisolator caps and contact bedding throughout the in-life portion of the study. Animals were provided with free access to a standard rodent chow and drinking water. The animal room was maintained under artificial lighting on a 12-h-light/dark cycle. Ambient temperature was maintained at 21°C \pm 3°C and humidity at 30%–80%.

Preparation of test articles

The stock solution of AAV5-hFVIII-SQ (2.98 \times 10¹³ vg/mL) was manufactured by Brammer Bio and purified and formulated by the

National Research Council, Canada. AAV5-hFVIII-SQ was used either undiluted or at a lower concentration using AAV5-hFVIII-SQ diluted with vehicle (10 mM sodium phosphate, 140 mM sodium chloride, 2% mannitol, 0.2% Pluronic F-68, pH 7.4). The vehicle was also used as the control treatment.

In-life procedures

Design of the study comparing different doses in neonates versus adults are summarized in [Figure S1A](#). Treatments were administered to 2-day-old neonates or at 8 weeks in adults. Adult mice ($n = 50$) were dosed with AAV5-hFVIII-SQ at 8 weeks of age at a dose of AAV5-hFVIII-SQ 3.5×10^{13} vg/kg (i.e., an absolute dose of 8.9×10^{11} vg/mouse) by tail vein. The neonatal group consisted of eight groups of ten 2-day-old mice. The mice received either the same absolute vector genomes as adults (i.e., 8.9×10^{11} vg/mouse; six cohorts) or the infusion based on body weight (i.e., 3.5×10^{13} vg/kg; two cohorts) by temporal vein, as described in previous work by Sands. In addition, 27 age-matched control male DKO mice were infused with vehicle at the age of 2 days and 1, 3, 5, 8, 11, 13, and 16 weeks of age. Adult mice that received AAV5-hFVIII-SQ were euthanized at 24 h or at 1, 3, 5, or 8 weeks after infusion. Neonatal mice that received AAV5-hFVIII-SQ were euthanized 24 h and 1, 3, 5, 8, and 16 weeks after infusion.

Design for the study comparing results in mice dosed at ages 1–8 weeks is summarized in [Figure S1B](#). Vector doses were selected such that all animals received approximately the same number of AAV5-hFVIII-SQ vector genomes based on the number delivered via a 6×10^{13} vg/kg infusion to 8-week old mice. DKO mice aged 2, 4, 6, and 8 days ($n = 10$ per group) were dosed with $\sim 1 \times 10^{12}$ AAV5-hFVIII-SQ, which corresponded to weight-adjusted doses of 1.5×10^{14} , 8.7×10^{13} , 6.5×10^{13} , and 6×10^{13} vg/kg, respectively. For 1-week old DKO mice, $\sim 7.5 \times 10^{11}$ of AAV5-hFVIII-SQ genomes were administered, corresponding to 2×10^{14} vg/kg. Additionally, 30 DKO mice were dosed with vehicle at different ages to match the ages of treated mice at take-down. Mice that received AAV5-hFVIII-SQ were euthanized 1, 2, 4, and 12 weeks post dose.

Sample collection

At various scheduled time points after study drug administration, each mouse was weighed and the body weight recorded. For the dose study, animals were anesthetized and exsanguinated by cardiac puncture. Blood was collected into tubes with 0.38% sodium citrate anticoagulant then centrifuged for 10 min under refrigeration (approximately 4°C at $1,500 \times g$ relative centrifugal force [RCF]). Due to volume constraints, plasma was collected into one tube for the 24-h neonatal group, while plasma was divided into two aliquots for all other animals. Plasma/red blood cells and buffy coat were stored at -80°C . Plasma hFVIII-SQ protein levels were measured at 24 h and 1, 3, 5, and 8 weeks after dosing in adult mice; at 24 h and 1, 3, 5, 8, and 16 weeks after infusion in neonatal mice; and at 24 h in vehicle-treated animals. For tissue collection from young mice, the livers were removed and divided into three equal pieces, with one piece formalin fixed and two pieces fresh frozen in liquid ni-

trogen. For the extraction of liver from older animals, the medial lobe was formalin fixed; the rest was divided into two aliquots, snap frozen in liquid nitrogen, and stored at -80°C . All samples for immunostaining were taken from the medial lobe.

In the study comparing mice dosed at ages 1–8 weeks, blood samples were collected from the inferior vena cava following euthanasia via carbon dioxide asphyxiation (mice aged 14 days through 70 days ± 1 day), or while under isoflurane/oxygen anesthesia followed by euthanasia and exsanguination (mice aged 84 days through 140 days ± 1 day). Blood samples were placed into tubes with 3.2% sodium citrate then centrifuged for 15 min under refrigeration (approximately 4°C at $2,800 \times g$ RCF). Plasma/red blood cells and buffy coat were stored at -80°C until analyses of FVIII protein level and protein activity. Whole liver was excised and weighed. Subsequently, representative samples of liver were separated for PCR and histological analyses.

Histology

All medial liver samples were fixed in 10% formalin for 48 h after collection. Subsequently, samples were switched to 70% ethanol immersion, placed flat in individual cassettes, and processed routinely for paraffin embedding within 1 month. Sections 5 μm thick were stained with hematoxylin and eosin and processed for immunohistochemical detection of hFVIII (1:500, ab139391; Abcam), BiP/GRP78 (1:200, C50B12; Cell Signaling Technology), HNF4 α (1:3,000, ab41898, Abcam), Ki-67 (1:800, ab16667, Abcam), and PHH3 (1:500, MABE939, Millipore). Anti-hFVIII antibody was detected using donkey anti-sheep IgG (H + L) cross-adsorbed secondary antibody conjugated to Alexa Fluor 488 (1:250, A-11015; Thermo Fisher Scientific). Anti-GRP78 antibody was detected using donkey anti-rabbit IgG (H + L) highly cross-adsorbed secondary antibody conjugated with Alexa Fluor 555 (1:500, A-31572; Thermo Fisher Scientific). Anti-HNF4 α antibody was detected using donkey anti-mouse (H + L) cross-adsorbed secondary antibody conjugated to Alexa Fluor 555 (1:500, A-31570; Thermo Fisher Scientific). Anti-Ki67 antibody was detected using donkey anti-rabbit (H + L) cross-adsorbed secondary antibody conjugated to Alexa Fluor 647 (1:500, A-31573; Thermo Fisher Scientific). Anti-PHH3 antibody was detected using donkey anti-rat (H + L) cross-adsorbed secondary antibody conjugated to Alexa Fluor 488 (1:250, A-21208; Thermo Fisher Scientific). Whole sections were scanned on a Zeiss Axio Scan.Z1 using a Plan-Apochromat 20 \times /0.8 objective with a Hamamatsu Orca Flash camera. Four images per animal and per group (with regions of interest including both central and portal veins) were analyzed to quantify the number of cells with elevated GRP78 signals. Because GRP78 is endogenously expressed in all hepatocytes, this quantification was designed to detect GRP78 immunofluorescence signal above the endogenous level. Hepatocytes staining positive for hFVIII-SQ protein, along with IHC intensity per cell, were quantified using Visiopharm image analysis software (Hoersholm, Denmark). Two images per animal and per group (with regions of interest selected including both central and portal veins) were used for quantification of HNF4 α , Ki-67 and PHH3. HNF4 α was used to label the nucleus of

hepatoblasts and hepatocytes.³⁵ Ki-67 was used to label the nucleus of cells in the active phases of the cell cycle (G1, S, G2, and M).³⁶ Labeling of PHH3 was used to visualize only the four actual phases of mitosis and late G2,³⁷ allowing for the distinction between cell proliferation and mitosis. The combination of these three markers allowed for the clear identification of the subpopulation of proliferating and mitotic hepatocytes.

Hepatocyte size was determined by outlining the cell membranes of 50 hepatocytes per age group per sample, as identified by a veterinary pathologist. The cross-sectional area of the outlined cells was measured in micrometers.

***In situ* hybridization to detect hFVIII-SQ DNA**

Formalin-fixed paraffin-embedded mouse liver sections (5 μ m) were collected on Superfrost Plus slides using RNase-free conditions. An RNAscope *in situ* hybridization protocol was performed using a Ventana Discovery Ultra Autostainer (Tucson, AZ), RNAscope (Newark, CA), Universal 2.5 Reagent Kit, and custom-generated hFVIII-SQ probes. Slides were counterstained with 4',6-diamidino-2-phenylindole and mounted with Fluoromount G. (catalog no. 17984–25, Electron Microscopy Sciences). Slides were imaged on an Axio Scan.Z1 (Zeiss) slide scanner using a Plan-Apochromat 20 \times /0.8 objective equipped with a Hamamatsu Orca Flash camera. Hepatocytes staining positive for hFVIII-SQ DNA, along with ISH intensity per cell, were quantified using Visiopharm image analysis software (Hoersholm, Denmark). The total number of positive hepatocytes was calculated using the following equations:

Total liver volume = liver weight/liver density

Volume of section analyzed = area of region of interest (ROI) \times section thickness.

ROI fraction of liver = volume of section analyzed/total liver volume.

Total positive hepatocytes = positive hepatocytes in ROI/ROI fraction of liver.

Total liver intensity = mean intensity per cell \times total positive cells.

Biochemical analysis

A total of 173 plasma samples were analyzed in duplicate wells for alanine aminotransferase and 152 were analyzed for hFVIII-SQ levels. A sandwich enzyme-linked immunosorbent assay was used to measure levels of hFVIII-SQ protein in sodium citrate-anticoagulated plasma. The assay used human-specific anti-FVIII capture (GMA-8023, Green Mountain Antibodies) and detection (F8C-EIA, Affinity Biologics) antibody pairs to specifically measure human FVIII and not endogenous mouse FVIII. Briefly, high-binding black polypropylene plates (Nunc MaxiSorp) were coated with 4 μ g/mL of anti-FVIII (domain A2) antibodies. Samples were diluted 1:10 in diluent buffer (6% bovine serum albumin in 1 \times tris-buffered saline with 0.1% [v/v] Tween 20) and incubated for approximately 1 h at ambient

temperature. hFVIII-SQ was detected by the addition of sheep anti-FVIII antibodies conjugated to horseradish peroxidase and incubated at ambient temperature for 1 h. After the final wash, QuantaBlu substrate solution (Thermo Scientific) was used for detection. The relative fluorescence units detected on the Molecular Devices FlexStation 3 instrument were proportional to the levels of hFVIII-SQ protein in the samples, and the concentrations were extrapolated from a standard curve. The 11-point standard curve was prepared by spiking in clinical-grade recombinant B-domain-deleted hFVIII (Xyntha) in hFVIII-deficient plasma (George King Biomedical) with the range of 0.684 to 700 ng/mL. The quantitative range for this assay was determined to be 2.73–700 ng/mL Xyntha (FVIII-SQ) in neat mouse plasma.

Quantitation of AAV5-hFVIII-SQ vector genome and hFVIII-SQ RNA transcript in liver

A total of 152 liver samples were analyzed in triplicate wells for total liver FVIII-SQ DNA and RNA. A liver fragment (\sim 20 mg) from each animal was homogenized at room temperature in 2-mL Lysing Matrix D tubes (MP Biomedicals) containing 600 μ L of RLT buffer (Qiagen). Total RNA and genomic DNA was extracted using the Qiagen DNA/RNA/Protein AllPrep kit following the manufacturer's instructions for manual extraction. Genomic DNA was eluted in 100 μ L of Qiagen elution buffer, and RNA was eluted in 100 μ L of nuclease-free water (Qiagen). The concentration of the extracted RNA and DNA was measured using a Nanodrop 2000 spectrophotometer (Thermo Scientific) using 2 μ L of samples. Each extracted DNA sample was diluted to 20 ng/ μ L and each RNA sample was diluted to 200 ng/ μ L.

Total levels of hFVIII-SQ vector genomes and RNA were measured from liver samples in triplicate with a quantitative PCR assay using probes and primers specific to the hFVIII-SQ transgene. The amount of hFVIII-SQ DNA and RNA were normalized to the quantity of input liver DNA, determined by absorbance at 260 nm using a spectrophotometer. The quantitative range for the method was 4.31×10^1 to 4.31×10^7 copies per reaction.

Identification of vector genome structures

The quantity of circular full-length vector genomes present as episomes and the proportion of concatemeric episomes were identified from DNA samples using restriction enzymes and ddPCR as previously described.¹⁸ Briefly, DNA samples were digested with PS-DNAse to eliminate all linear DNA species (including genomic DNA) and enrich circular genomes. The samples were then used in ddPCR reactions, which capture a single DNA molecule (either a monomer or concatemer) and thus quantify the number of circular genomes present in the sample. In parallel, the PS-DNAse-treated DNA samples were also treated with the restriction enzyme KpnI, which cuts once within the vector genome unit, thus separating individual vector genome units within the circular genomes. These doubly treated DNA samples were then used in ddPCR reactions. The presence of concatemers was inferred if there were increases in the levels of vector genome upon KpnI digestion compared with the number of circular genomes identified with only PS-DNAse

treatment. Southern blotting was then used to identify the presence of monomers, dimers, and trimers and the orientation of vector genome units within concatemers as previously described.¹⁸

Statistical analyses

Statistical comparisons between treatment groups were conducted using one-way analysis of variance (ANOVA) followed by Dunnett's or Tukey's multiple comparison test. Comparisons between FVIII production and secretion in neonatal versus adult mice at multiple time points were performed with a two-way ANOVA using a Sidak's multiple comparison. Statistical analyses were performed using Prism (v 9.0.2, GraphPad).

Distribution of materials and data

Materials and protocols will be distributed to qualified scientific researchers for non-commercial, academic purposes. The AAV5-hFVIII-SQ vector and the AAV5-hFVIII-SQ vector sequence are part of an ongoing development program, and they will not be shared.

SUPPLEMENTAL INFORMATION

Supplemental information can be found online at <https://doi.org/10.1016/j.omtm.2022.08.002>.

ACKNOWLEDGMENTS

Funding for this study was provided by BioMarin Pharmaceutical Inc. Elli Koziol of BioMarin Pharmaceutical Inc. contributed to the biochemical and molecular analyses. Medical writing and editorial support were provided by Kathleen Pieper, PhD, and Atreju Lackey, PhD, of AlphaBioCom, LLC, and funded by BioMarin Pharmaceutical Inc.

AUTHOR CONTRIBUTIONS

S.F., S. Bullens, S. Bunting, C.F., C.O., and S.S. contributed to the study design. A.C., W.Z., C.S., S.C., and J.H. performed the statistical analyses. L.Z., R.M., L.X., and J.A. contributed to animal studies. B.H., C.-R.S., S.L., C.V., A.V.T., T.B., and J.H. performed the biochemical and molecular analyses. S.C., N.G., B.Y., and D.T. performed the histologic analyses. All authors critically reviewed the manuscript and contributed to interpretation of the data.

DECLARATION OF INTERESTS

L.Z., B.Y., B.H., C.-R.S., S.F., S. Bunting, S. Bullens, R.M., L.X., J.A., J.H., A.V.T., T.B., J.H., C.V., D.T., C.S., and C.O. are employees and stockholders of BioMarin Pharmaceutical Inc. W.Z., S.S., N.G., A.C., S.L., C.F., S.C., and J.S. are former employees of BioMarin Pharmaceutical Inc. and may hold stock.

REFERENCES

- Srivastava, A., Santagostino, E., Dougall, A., Kitchen, S., Sutherland, M., Pipe, S.W., Carcao, M., Mahlangu, J., Ragni, M.V., Windyga, J., et al. (2020). WFH guidelines for the management of hemophilia, 3rd edition. *Haemophilia* 26 (Suppl 6), 1–158.
- Srivastava, A., Brewer, A.K., Mauser-Bunschoten, E.P., Key, N.S., Kitchen, S., Llinas, A., Ludlam, C.A., Mahlangu, J.N., Mulder, K., Poon, M.C., et al. (2013). Guidelines for the management of hemophilia. *Haemophilia* 19, 1–47.
- Llinás, A. (2010). Haemophilic arthropathy. *Haemophilia* 16 (Suppl 5), 121.
- Rodriguez-Merchan, E.C. (2010). Musculoskeletal complications of hemophilia. *HSS J.* 6, 37–42.
- Bertamino, M., Riccardi, F., Banov, L., Svahn, J., and Molinari, A.C. (2017). Hemophilia care in the pediatric age. *J. Clin. Med.* 6, E54.
- Manco-Johnson, M.J., Abshire, T.C., Shapiro, A.D., Riske, B., Hacker, M.R., Kilcoyne, R., Ingram, J.D., Manco-Johnson, M.L., Funk, S., Jacobson, L., et al. (2007). Prophylaxis versus episodic treatment to prevent joint disease in boys with severe hemophilia. *N. Engl. J. Med.* 357, 535–544.
- Manco-Johnson, M.J., Lundin, B., Funk, S., Peterfy, C., Raunig, D., Werk, M., Kempton, C.L., Reding, M.T., Goranov, S., Gercheva, L., et al. (2017). Effect of late prophylaxis in hemophilia on joint status: a randomized trial. *J. Thromb. Haemost.* 15, 2115–2124.
- Den Uijl, I.E.M., Mauser Bunschoten, E.P., Roosendaal, G., Schutgens, R.E.G., Biesma, D.H., Grobbee, D.E., and Fischer, K. (2011). Clinical severity of haemophilia A: does the classification of the 1950s still stand? *Haemophilia* 17, 849–853.
- Rangarajan, S., Walsh, L., Lester, W., Perry, D., Madan, B., Laffan, M., Yu, H., Vettermann, C., Pierce, G.F., Wong, W.Y., and Pasi, K.J. (2017). AAV5-factor VIII gene transfer in severe hemophilia A. *N. Engl. J. Med.* 377, 2519–2530.
- Pasi, K.J., Rangarajan, S., Mitchell, N., Lester, W., Symington, E., Madan, B., Laffan, M., Russell, C.B., Li, M., Pierce, G.F., and Wong, W.Y. (2020). Multiyear follow-up of AAV5-hFVIII-SQ gene therapy for hemophilia A. *N. Engl. J. Med.* 382, 29–40.
- Pasi, K.J., Laffan, M., Rangarajan, S., Robinson, T.M., Mitchell, N., Lester, W., Symington, E., Madan, B., Yang, X., Kim, B., et al. (2021). Persistence of haemostatic response following gene therapy with valoctocogene roxaparvovec in severe hemophilia A. *Haemophilia* 27, 947–956.
- Branchford, B.R., Monahan, P.E., and Di Paola, J. (2013). New developments in the treatment of pediatric hemophilia and bleeding disorders. *Curr. Opin. Pediatr.* 25, 23–30.
- Wang, L., Wang, H., Bell, P., McMenamin, D., and Wilson, J.M. (2012). Hepatic gene transfer in neonatal mice by adeno-associated virus serotype 8 vector. *Hum. Gene Ther.* 23, 533–539.
- Wang, L., Bell, P., Lin, J., Calcedo, R., Tarantal, A.F., and Wilson, J.M. (2011). AAV8-mediated hepatic gene transfer in infant rhesus monkeys (*Macaca mulatta*). *Mol. Ther.* 19, 2012–2020.
- Han, S.O., Li, S., McCall, A., Arnson, B., Everitt, J.I., Zhang, H., Young, S.P., ElMallah, M.K., and Koeberl, D.D. (2020). Comparisons of infant and adult mice reveal age effects for liver depot gene therapy in pompe disease. *Mol. Ther. Methods Clin. Dev.* 17, 133–142.
- Binny, C., McIntosh, J., Della Peruta, M., Kymalainen, H., Tuddenham, E.G.D., Buckley, S.M.K., Waddington, S.N., McVey, J.H., Spence, Y., Morton, C.L., et al. (2012). AAV-mediated gene transfer in the perinatal period results in expression of FVII at levels that protect against fatal spontaneous hemorrhage. *Blood* 119, 957–966.
- Bunting, S., Zhang, L., Xie, L., Bullens, S., Mahimkar, R., Fong, S., Sandza, K., Harmon, D., Yates, B., Handyside, B., et al. (2018). Gene therapy with BMN 270 results in therapeutic levels of FVIII in mice and primates and normalization of bleeding in hemophilic mice. *Mol. Ther.* 26, 496–509.
- Sihn, C.R., Handyside, B., Liu, S., Zhang, L., Murphy, R., Yates, B., Xie, L., Torres, R., Russell, C.B., O'Neill, C.A., et al. (2022). Molecular analysis of AAV5-hFVIII-SQ vector-genome-processing kinetics in transduced mouse and nonhuman primate livers. *Mol. Ther. Methods Clin. Dev.* 24, 142–153.
- Konkle, B.A., Stine, K., Visweshwar, N., Harrington, T., Leavitt, A.D., Arkin, S., Di Russo, G., Conner, E., and Rouy, D. (2019). OC 01.2 Initial results of the Alta study, a phase 1/2, open label, adaptive, dose-ranging study to assess the safety and tolerability of SB-525 gene therapy in adult subjects with severe hemophilia A [abstract]. *Res Pract Thromb Haemost* 3, 80.
- Nakai, H., Storm, T.A., and Kay, M.A. (2000). Recruitment of single-stranded recombinant adeno-associated virus vector genomes and intermolecular recombination are responsible for stable transduction of liver in vivo. *J. Virol.* 74, 9451–9463.

21. McClements, M.E., and MacLaren, R.E. (2017). Adeno-associated virus (AAV) dual vector strategies for gene therapy encoding large transgenes. *Yale J. Biol. Med.* *90*, 611–623.
22. Srivastava, A. (2016). Advances and challenges in the use of recombinant AAV vectors for human gene therapy. *Cell Gene Ther. Insights* *2*, 553–575.
23. Wu, Z., Yang, H., and Colosi, P. (2010). Effect of genome size on AAV vector packaging. *Mol. Ther.* *18*, 80–86.
24. Fong, S., Handyside, B., Sihn, C.R., Liu, S., Zhang, L., Xie, L., Murphy, R., Galicia, N., Yates, B., Minto, W.C., et al. (2020). Induction of ER stress by an AAV5 BDD FVIII construct is dependent on the strength of the hepatic-specific promoter. *Mol. Ther. Methods Clin. Dev.* *18*, 620–630.
25. Halpern, K.B., Shenhav, R., Matcovitch-Natan, O., Toth, B., Lemze, D., Golan, M., Massasa, E.E., Baydatch, S., Landen, S., Moor, A.E., et al. (2017). Single-cell spatial reconstruction reveals global division of labour in the mammalian liver. *Nature* *542*, 352–356.
26. Chang, M., Parker, E.A., Muller, T.J.M., Haenen, C., Mistry, M., Finkelstein, G.P., Murphy-Ryan, M., Barnes, K.M., Sundaram, R., and Baron, J. (2008). Changes in cell-cycle kinetics responsible for limiting somatic growth in mice. *Pediatr. Res.* *64*, 240–245.
27. Arrojo e Drigo, R., Lev-Ram, V., Tyagi, S., Ramachandra, R., Deerinck, T., Bushong, E., Phan, S., Orphan, V., Lechene, C., Ellisman, M.H., and Hetzer, M.W. (2019). Age mosaicism across multiple scales in adult tissues. *Cell Metab.* *30*, 343–351.e3.
28. Cunningham, S.C., Dane, A.P., Spinoulas, A., and Alexander, I.E. (2008). Gene delivery to the juvenile mouse liver using AAV2/8 vectors. *Mol. Ther.* *16*, 1081–1088.
29. Lee, E.K., Hu, C., Bhargava, R., Rozengurt, N., Stout, D., Grody, W.W., Cederbaum, S.D., and Lipshutz, G.S. (2012). Long-term survival of the juvenile lethal arginase-deficient mouse with AAV gene therapy. *Mol. Ther.* *20*, 1844–1851.
30. Chandler, R.J., LaFave, M.C., Varshney, G.K., Trivedi, N.S., Carrillo-Carrasco, N., Senac, J.S., Wu, W., Hoffmann, V., Elkhouloun, A.G., Burgess, S.M., and Venditti, C.P. (2015). Vector design influences hepatic genotoxicity after adeno-associated virus gene therapy. *J. Clin. Invest.* *125*, 870–880.
31. Wang, P.R., Xu, M., Toffanin, S., Li, Y., Llovet, J.M., and Russell, D.W. (2012). Induction of hepatocellular carcinoma by in vivo gene targeting. *Proc. Natl. Acad. Sci. USA* *109*, 11264–11269.
32. Donsante, A., Miller, D.G., Li, Y., Vogler, C., Brunt, E.M., Russell, D.W., and Sands, M.S. (2007). AAV vector integration sites in mouse hepatocellular carcinoma. *Science* *317*, 477.
33. Dalwadi, D.A., Torrens, L., Abril-Fornaguera, J., Pinyol, R., Willoughby, C., Posey, J., Llovet, J.M., Lanciault, C., Russell, D.W., Grompe, M., and Naugler, W.E. (2021). Liver injury increases the incidence of HCC following AAV gene therapy in mice. *Mol. Ther.* *29*, 680–690.
34. Miao, H.Z., Sirachainan, N., Palmer, L., Kucab, P., Cunningham, M.A., Kaufman, R.J., and Pipe, S.W. (2004). Bioengineering of coagulation factor VIII for improved secretion. *Blood* *103*, 3412–3419.
35. Gordillo, M., Evans, T., and Gouon-Evans, V. (2015). Orchestrating liver development. *Development* *142*, 2094–2108.
36. Scholzen, T., and Gerdes, J. (2000). The Ki-67 protein: from the known and the unknown. *J. Cell. Physiol.* *182*, 311–322.
37. Hendzel, M.J., Wei, Y., Mancini, M.A., Van Hooser, A., Ranalli, T., Brinkley, B.R., Bazett-Jones, D.P., and Allis, C.D. (1997). Mitosis-specific phosphorylation of histone H3 initiates primarily within pericentromeric heterochromatin during G2 and spreads in an ordered fashion coincident with mitotic chromosome condensation. *Chromosoma* *106*, 348–360.